An ^{18}F-Labeled PSMA Ligand for PET/CT of Prostate Cancer: First-in-Humans Observational Study and Clinical Experience with ^{18}F-JK-PSMA-7 During the First Year of Application

Felix Dietlein[1,2], Melanie Hohberg[1], Carsten Kobe[1], Boris D. Zlatopolskiy[3], Philipp Krapf[4], Heike Endepols[1,3], Philipp Täger[1], Jochen Hammes[1], Axel Heidenreich[5], Bernd Neumaier*[3,4], Alexander Drzezga*[1], and Markus Dietlein*[1]

[1]Department of Nuclear Medicine, University Hospital of Cologne, Cologne, Germany; [2]Department of Medical Oncology, Dana-Farber Cancer Institute, Harvard Medical School, Boston, Massachusetts; [3]Institute of Radiochemistry and Experimental Molecular Imaging, University Hospital of Cologne, Cologne, Germany; [4]INM-5: Nuclear Chemistry, Institute of Neuroscience and Medicine, Forschungszentrum Jülich, Jülich, Germany; and [5]Department of Urology, University Hospital of Cologne, Cologne, Germany

In preclinical trials, the recently developed tracer 2-methoxy-^{18}F-DCFPyL (^{18}F-JK-prostate-specific membrane antigen [PSMA]-7) has shown favorable properties regarding clinical performance and radiochemical accessibility. The aim of this study was to evaluate the clinical utility of ^{18}F-JK-PSMA-7 for PET/CT imaging of patients with prostate cancer. **Methods:** In an Institutional Review Board–approved pilot study, the initial clinical utility of PET/CT imaging with ^{18}F-JK-PSMA-7 was directly compared with ^{68}Ga-PSMA-11 PET/CT in a group of 10 patients with prostate cancer. The 2 PSMA tracers were administered to each patient less than 3 wk apart. Next, we analyzed the data of 75 consecutive patients who had undergone clinical ^{18}F-JK-PSMA-7 PET/CT imaging for tumor localization of biochemical recurrence (BCR). **Results:** The pilot study in 10 patients who were examined with both PSMA tracers demonstrated that ^{18}F-JK-PSMA-7 was at least equivalent to ^{68}Ga-PSMA-11. All unequivocally ^{68}Ga-PSMA-11–positive lesions could be also detected using ^{18}F-JK-PSMA-7, and in 4 patients additional suspected PSMA-positive lesions were identified (1 patient changed from PSMA-negative to PSMA-positive). In patients with BCR (after prostatectomy or radiotherapy), the capacity of ^{18}F-JK-PSMA-7 PET/CT to detect at least one PSMA-positive lesion was 84.8%. The prostate-specific antigen (PSA)–stratified detection rate of ^{18}F-JK-PSMA-7 after prostatectomy varied among 54.5% (6/11 patients; PSA < 0.5 μg/L), 87.5% (14/16 patients; PSA 0.5–2 μg/L), and 90.9% (20/22 patients; PSA > 2 μg/L). **Conclusion:** The tracer ^{18}F-JK-PSMA-7 was found to be safe and clinically useful. We demonstrated that ^{18}F-JK-PSMA-7 was not inferior when directly compared with ^{68}Ga-PSMA-11 in a pilot study but indeed identified additional PSMA-avid suspected lesions in oligometastasized patients with BCR. In a subsequent analysis of a clinical cohort of BCR patients, ^{18}F-JK-PSMA-7 was useful in tumor localization. ^{18}F-JK-PSMA-7 is recommended for future prospective trials.

When a patient experiences a new increase in prostate-specific antigen (PSA) levels after surgery or radiation therapy for prostate cancer, commonly referred to as biochemical recurrence (BCR), sensitive imaging modalities are needed to decide on metastasis-directed therapy options (*1,2*). Over the past few years, radiolabeled PSMA–specific PET tracers have been increasingly used to localize prostate cancer (*3–9*). The rationale behind these tracers is the fact that tumor cells display an approximately 8- to 12-fold increased expression of folate hydrolase 1, better known as prostate-specific membrane antigen (PSMA), on their surface, compared with noncancerous prostate tissue (*10,11*). An additional advantage of PSMA-specific PET tracers is that they are not negatively affected by therapies targeting the signaling of the androgen receptor in castration-resistant prostate cancer (*12*).

Most PET tracers currently established for cancer detection are labeled with ^{18}F because of its ideal decay properties regarding half-life, availability from a cyclotron, and high image resolution due to its low β^+-emission energy (*13,14*). However, regarding PSMA ligands, ^{68}Ga-labeled compounds were the first widely used in clinical studies (*15*). Advantages are that no access to a cyclotron is required and that ^{68}Ga-labeled tracers can easily be obtained without complex radiosynthetic chemistry, since the ^{68}Ga label can be introduced by simple complex formation with an appropriate chelator (*16*). In 2011, Chen et al. reported on synthesis of the ^{18}F-labeled PSMA-specific tracer 2-(3-{1-carboxy-5-[(6-^{18}F-fluoro-pyridine-3-carbonyl)-amino]-pentyl}-ureido)-pentanedioic acid (^{18}F-DCFPyL) using a multistep protocol that involved radiofluorination of a prosthetic group (*17*). Clinical studies revealed that ^{18}F-DCFPyL displayed at least noninferior sensitivity in detecting relapsed tumors in prostate cancer patients, compared with ^{68}Ga-PSMA-11 (*6,7,18,19*). In some patients, these tracers even exhibited increased sensitivity, possibly due to the increased

resolution of the ^{18}F label for small anatomic structures such as small iliac lymph nodes.

When ^{18}F-labeled PSMA ligands were introduced into the clinical setting, their synthesis was far more difficult than that of their ^{68}Ga-labeled counterparts in routine clinical practice (*17,20*). Indeed, if the synthesis reaction of ^{18}F-DCFPyL is not performed under optimal conditions, an unstable isomer is formed, which leads to rapid defluorination of the ^{18}F-labeled PSMA-specific product (*21,22*).

Recently, our group introduced the PSMA-specific derivative 2-methoxy-^{18}F-DCFPyL (^{18}F-JK-PSMA-7), a new compound for PET imaging. This compound had been selected from a group of several candidates because of its favorable imaging properties (*23*). The abbreviation JK (J for Jülich and K for Köln [Cologne]) refers to the Forschungszentrum Jülich and the University Hospital of Cologne, which were involved in the development of this tracer. In addition, we recently reported on a minimalist approach that enables us to implement a robust and high-yielding process for synthesizing ^{18}F-JK-PSMA-7, with minor variations in release specifications ideally suited for high-throughput production in a clinical setting (*23*).

Here, we present the first application of ^{18}F-JK-PSMA-7 in a pilot study, demonstrating its noninferiority to the benchmark tracer ^{68}Ga-PSMA-11. Furthermore, we report the results of the first routine clinical application of this tracer in a cohort of 75 prostate cancer patients with BCR.

MATERIALS AND METHODS

Study Design and Patient Selection Criteria

In brief, our study followed a 2-step approach. In the first step, we offered an additional ^{18}F-JK-PSMA-7 PET/CT scan to 10 patients who had undergone ^{68}Ga-PSMA-11 imaging. Nine of these 10 patients had recently experienced BCR of their disease, and 1 patient with known oligometastatic status showed a raised PSA level. The ^{68}Ga-PSMA-11 scans were interpreted as negative or inconclusive in 5 patients; only a solitary PSMA lesion had been detected in the other 5 patients. To improve the certainty of the assumed tumor localization or to exclude any additional PSMA-positive metastases, we performed a second PET/CT scan with ^{18}F-JK-PSMA-7 within 3 wk of the ^{68}Ga-PSMA-11 scan. The rationale was our previous experience indicating a potentially superior detection rate for ^{18}F-labeled PSMA-specific PET tracers (*7,18*). We did not observe any adverse side effects in any of those 10 patients during the entire examination procedure (up to 3 h after injection of ^{18}F-JK-PSMA-7). Furthermore, in telephone counseling on therapeutic options some weeks later, none of the patients reported any new side effects.

In the second step, we used the novel ^{18}F-JK-PSMA-7 tracer to examine a cohort of 75 prostate cancer patients with BCR who were referred to our institute for PET/CT imaging between March 2017 and December 2017. Of these patients, 49 presented with BCR after surgery, 47 of whom had a PSA level of at least 0.2 μg/L after nadir. The other 26 patients of the 75-patient cohort presented with BCR after radiotherapy (external-beam radiation therapy, brachytherapy, seed implantation). Seventeen of these patients had a PSA level of at least 2 μg/L after nadir. The other 9 patients had a PSA increase of less than 2 μg/L and did not fulfill the Phoenix criterion for BCR but nevertheless were referred for restaging because of continuously rising PSA values with no sign of intraprostatic inflammation.

The institutional review board approved this retrospective study, and all subjects gave written informed consent. All procedures were performed in compliance with the regulations of the responsible local authorities (District Administration of Cologne, Germany).

Imaging

Patients fasted for approximately 4 h before undergoing PET/CT to allow administration of contrast agent when neither CT scans nor MRI scans had been performed previously and to exclude any interference with the novel ^{18}F-JK-PSMA-7. Data on ^{18}F-DCFPyL had previously shown that fasting did not influence PSMA accumulation in metastases (*24*), but we had no data on the influence of fasting on ^{18}F-JK-PSMA-7 uptake. In our pilot study, a mean dose of 141 ± 30 MBq of ^{68}Ga-PSMA-11 and a mean dose of 358 ± 15 MBq of ^{18}F-JK-PSMA-7 were injected. Following previously published protocols, ^{68}Ga-PSMA-11 PET scans were acquired 1 h after injection (*3–5*). In patients with a PSA level below 2.0 μg/L, a second scan of the pelvis and lower abdomen was performed 3 h after injection, to guarantee maximal sensitivity for the ^{68}Ga-PSMA-11 tracer (*25–28*). In parallel with previous studies using ^{18}F-DCFPyL (*6,7*), ^{18}F-JK-PSMA-7 PET scans were acquired 2 h after tracer injection. In the pilot study, we additionally generated a series of PET data between 10 and 230 min after injection in 9 of our 10 patients, to define the scans with the best visualization of the PSMA-positive tissue (*29*). All images were acquired on a Biograph mCT 128 Flow PET/CT scanner (Siemens Healthineers). The same filters and acquisition times (15 min from top of skull to mid thigh) were used for ^{68}Ga-PSMA-11 1 h after the injection and for ^{18}F-JK-PSMA-7. The second ^{68}Ga-PSMA-11 PET scan had a FlowMotion (Siemens) bed speed of 0.7 mm/s instead of 1.5 mm/s to compensate for the decay of ^{68}Ga-PSMA-11. Non–contrast-enhanced (low-dose) CT scans were conducted in parallel with PET imaging. Images were reconstructed using an ultrahigh-definition algorithm (*13*).

All PET scans were analyzed by a team of at least 2 specialists in nuclear medicine and 1 radiologist. A scan was scored as positive if focal tracer accumulation was detected in the prostate fossa, in a lymph node, or at a distant site. A focus of tracer accumulation was interpreted as a suspected lymph node if it showed a morphologic correlate on the corresponding CT scan consistent with a regional lymph node, even when the diameter was less than 8 mm. The PET/CT reading was performed according to the published criteria for harmonization of the PSMA PET/CT interpretation (*30,31*).

Tracer Preparation

All tracers were synthesized in accordance with applicable good manufacturing practices using a 2-step protocol. Additionally, extensive quality control measures, including radiochemical purity, endotoxin testing, pH, and determination of residual solvents such as acetonitrile, acetone, tertiary butanol, and tetraethylammonium hydrogen carbonate, were performed.

In brief, ^{18}F-JK-PSMA-7 was prepared using a 2-step reaction. In the first step, the radiolabeled active ester was produced by the nucleophile reaction of ^{18}F with 2-methoxy-*N,N,N*-trimethyl-5-((2,3,5,6-tetrafluorophenoxy) carbonyl) pyridine-2-aminium-trifluoromethanesulfonate to generate the ester 2,3,5,6-tetrafluorophenyl-6-(^{18}F-fluoro)-4-methoxy-nicotinate (^{18}F-FPy-OMe-TFP). In the second step, 4.6 ± 0.1 mg of (((*S*)-5-amino-1-carboxypentyl)-carbamoyl)-L-glutamic-acid was added to ^{18}F-FPy-OMe-TFP and subsequently incubated at 45°C for 6 min. Then, the final product, ^{18}F-JK-PSMA-7, was purified by solid-phase extraction (Oasis HLB; Waters) and formulated in saline. This reaction provided ^{18}F-JK-PSMA-7 in a high radiochemical yield of up to 40% and a high radiochemical purity (>95%). The specific concentration of F-PSMA-7 was no more than 10 μg/mL. The upper limit of the injected volume was 10 mL; the activity of ^{18}F-JK-PSMA-7 was at least 30 MBq/mL. Each week, we produced 2 batches of ^{18}F-JK-PSMA-7. The detailed procedure for the radiosynthesis using the minimalist light protocol is described elsewhere (*23*). The activity produced and the radiochemical purity were analyzed for the 74 consecutive batches of ^{18}F-JK-PSMA-7 synthesized within the first year of clinical application.

Synthesis of 68Ga-PSMA-11 was performed as described previously (*32,33*).

RESULTS

Robustness and Reliability of 18F-JK-PSMA-7 Production

We analyzed the quality of 74 consecutive synthesis batches of 18F-JK-PSMA-7 over the course of 12 mo. We found a high radiochemical activity per synthesis (mean activity, 6,660 MBq ± 2,869 MBq; interquartile range, 2,712 MBq) and a high radiochemical purity (mean purity, 98.6% ± 1.6%; interquartile range, 2.4%). In the course of this study, only 2 of 74 syntheses (2.7%) failed to reach a radiochemical purity of more than 95%.

Direct Comparison Between the Biodistribution Patterns of 18F-JK-PSMA-7 and 68Ga-PSMA-11

We next assessed the validity of 18F-JK-PSMA-7. For this purpose, we offered 10 patients who had just undergone PET/CT imaging with 68Ga-PSMA-11 an additional PET/CT scan with 18F-JK-PSMA-7. We performed the second PET/CT scan within less than 3 wk and found that all unequivocally 68Ga-PSMA-11–positive lesions could be validated using 18F-JK-PSMA-7. Moreover, 4 patients displayed at least 1 suspected PSMA-positive lesion on the 18F-JK-PSMA-7 scan that had been missed by 68Ga-PSMA-11 (Figs. 1–4). Intriguingly, in 3 of these 4 patients, the additional PSMA-positive lesions were located in locoregional lymph nodes (iliac lymph nodes: patients 2 and 4; retroperitoneal lymph nodes: patient 7). In 1 patient (patient 1), a PSMA-positive bone lesion that was revealed by 18F-JK-PSMA-7 had been known from the 18F-DCFPyL PET/CT scan 2 y before.

The follow-up data of the 10 patients are summarized in Tables 1 and 2. First, we report the details of the 4 patients with the different PET findings. In 1 of these patients (patient 4), the first PET/CT scan with 68Ga-PSMA-11 was interpreted as completely negative. The PSMA-positive left iliac lymph node that was detected by 18F-JK-PSMA-7 was a plausible explanation for the BCR in patient 4, with a PSA level of 1.1 ng/mL, and was finally confirmed by tumor growth seen on an externally performed 68Ga-PSMA-11 PET/CT examination 8 mo later. The salvage lymphadenectomy initially undertaken could not verify the PET finding. The PSMA-positive lymph nodes found additionally by the 18F-JK-PSMA-7 scan in 2 other patients (patients 2 and 7) were localized in the same lymph node area as that in which the 68Ga-PSMA-11 PET/CT had already depicted 1 PSMA-positive lymph node. Both patients received radiotherapy of the PSMA-positive lymph node area, and the PSA level dropped after the irradiation.
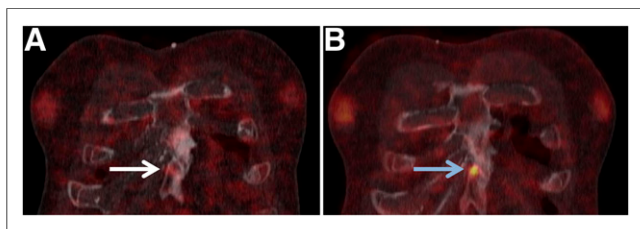

FIGURE 1. 68Ga-PSMA-11 PET/CT (A) and 18F-JK-PSMA-7 PET/CT (B) of patient 1. Besides concordant PSMA-positive tissue within irradiated prostate (not shown), patient had previously proven bone metastases, appearing positive in sternum on 18F-JK-PSMA-7 scan (arrow) but only faintly positive on 68Ga-PSMA-11 scan (arrow).
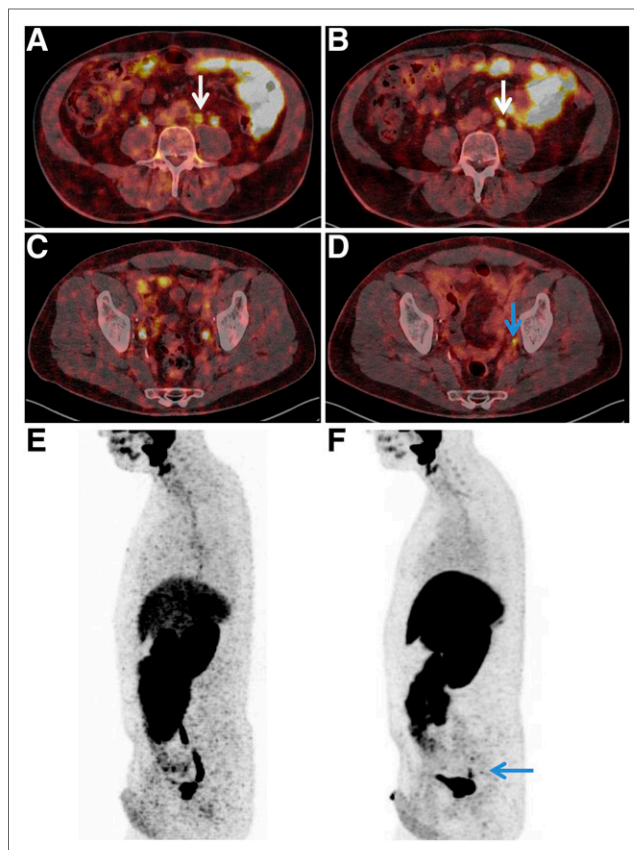
FIGURE 2. 68Ga-PSMA-11 PET/CT (A, C, and E) and 18F-JK-PSMA-7 PET/CT (B, D, and F) of patient 2. Besides concordant PSMA-positive lymph node on left near bifurcation (arrows on A and B), 18F-JK-PSMA-7 in this patient revealed small PSMA-positive left iliac caudal lymph node dorsal to ureter (arrows on D and F).

Second, we observed concordant findings using both PSMA tracers in 6 patients: concordantly positive in 2 patients (patients 5 and 11) and concordantly negative in 4 patients (patients 3, 7, 9, and 10).
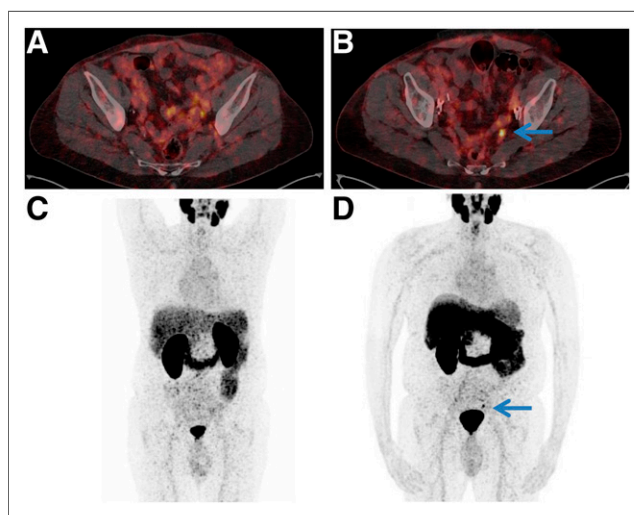

FIGURE 3. 68Ga-PSMA-11 PET/CT (A and C) and 18F-JK-PSMA-7 PET/CT (B and D) of patient 4. PSMA-positive left iliac lymph node was visible on 18F-JK-PSMA-7 PET/CT (arrows).
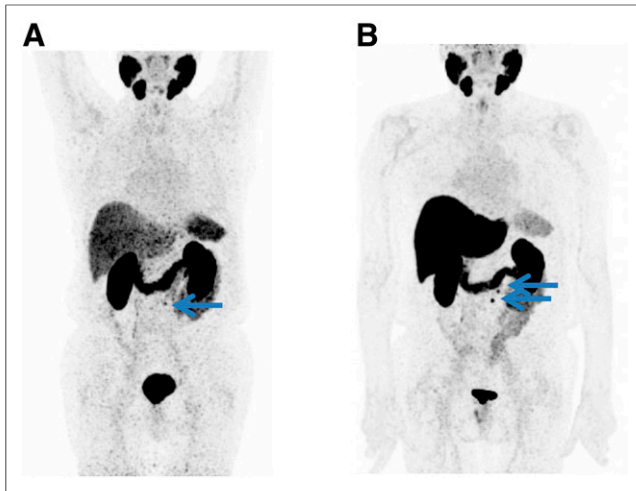
FIGURE 4. ^{68}Ga-PSMA-11 PET/CT (A) and ^{18}F-JK-PSMA-7 PET/CT (B) maximum-intensity projections of patient 7. ^{68}Ga-PSMA-11 PET/CT revealed only 1 PSMA-positive retroperitoneal paraaortic lymph node (arrow on A), whereas ^{18}F-JK-PSMA-7 PET/CT showed 2 PSMA-positive retroperitoneal lymph nodes (arrows on B).

Both PSMA-positive patients showed PSMA-positive tissue within the prostate fossa and received salvage radiotherapy. One of the 4 PSMA-negative patients was subjected to salvage radiotherapy of the prostate fossa.

Benchmarking the Detection Rate of ^{18}F-JK-PSMA-7 Across 75 Prostate Cancer Patients with BCR

Closing the pilot study, we examined 162 prostate cancer patients with ^{18}F-JK-PSMA-7 (349 ± 53 MBq) within a year of the clinical application of ^{18}F-JK-PSMA-7. Focusing on the localization of BCR as the main indication for PET/CT, we studied the detection rate of ^{18}F-JK-PSMA-7 (347 ± 56 MBq) in 75 patients, aged 69.2 ± 8.1 y, with increasing PSA levels after initial curative treatment, for whom it was unclear whether they carried PSMA-positive lesions (Table 3). These patients did not receive androgen deprivation therapy. We analyzed the detection rate separately for patients after prostatectomy with or without salvage radiotherapy versus patients after radiotherapy alone.

Overall, 49 patients in our cohort had recently experienced BCR after prostatectomy with or without salvage radiotherapy. In 40 of these prostatectomy patients, we detected ^{18}F-JK-PSMA-7–positive lesions, resulting in a detection rate of 81.6%. The PSA-stratified detection rate for ^{18}F-JK-PSMA-7 varied among 54.5% (6/11 patients; PSA < 0.5 μg/L), 87.5% (14/16 patients; PSA 0.5–2 μg/L), and 90.9% (20/22 patients; PSA > 2 μg/L).

Our cohort contained a further group of 26 patients who presented with a PSA increase after radiotherapy. The detection rate for the ^{18}F-JK-PSMA-7 tracer was 94.1% (16/17) in patients with BCR according to the Phoenix criterion (PSA level ≥ 2.0 μg/L above nadir). Some patients were referred for PSMA PET/CT when the PSA increase was repeatedly confirmed but remained below 2.0 μg/L and the Phoenix criterion defining the BCR had not yet been reached. In this constellation, the ^{18}F-JK-PSMA-7 PET scan detected PSMA-positive tissue in 33.3% of patients (3/9).

Tumor relapse patterns substantially differed between BCR patients after surgery and BCR patients after radiotherapy. Although 19 of the 49 prostatectomy patients (38.8%) displayed PSMA positivity exclusively in lymph nodes, this pattern was rarely observed in the patients with a PSA increase after radiotherapy (3/26, 11.5%). Several of the radiotherapy patients, however, displayed PSMA-positive tissue exclusively within the prostate (8/26, 30.8%).

Verification

After the introduction of ^{18}F-JK-PSMA-7 into our clinical care procedures, collection of data on verification became part of our quality assurance program. After an interval of 6–18 mo, we read all the written reports, which were sent to our institute. Additionally, we checked all our electronic patient files.

The PSMA-positive lesions in the 59 patients who underwent PET/CT for BCR were confirmed by histology in 6 patients, by follow-up in 17 patients, and by morphologic imaging in 20 patients. Further information was missing for 16 patients. The histologic verification resulted from salvage lymphadenectomies with PSMA-positive lymph node metastases. Verification by follow-up was based on a decrease in PSA level after radiotherapy (n = 9), progression of the PSMA-positive lesion after watchful waiting (n = 7), or regression of the PSMA-positive lesion after starting ADT (n = 1). One of these patients with progressive PSMA-positive nodal disease on a second PET exam had shown positive ^{18}F-JK-PSMA-7 PET/CT findings but then negative histologic results (0/14 lymph nodes) after salvage lymphadenectomy. We therefore did not interpret this ^{18}F-JK-PSMA-7 PET/CT finding as false-positive. The verification by morphologic imaging summarized patients in whom CT demonstrated an osteosclerotic or osteolytic lesion (n = 11), a suspected lymph node at least 8 mm in diameter within the pelvis (n = 7), or a suspected pulmonary lesion (n = 1) and patients in whom MRI had revealed a suggestive lesion within the prostate (n = 1).

DISCUSSION

Over the past 4 y, we have successfully introduced ^{18}F-DCFPyL and later ^{18}F-JK-PSMA-7 into our routine PET/CT imaging procedure for prostate cancer patients (7,18,34). We described the synthesis of ^{18}F-JK-PSMA-7 and found that it could be produced with a consistently high radiochemical yield and purity (23). This robust synthesis substantially reduced the need to reschedule appointments at short notice in our institute. Furthermore, recent preclinical data have highlighted favorable properties of ^{18}F-JK-PSMA-7 in comparison with other ^{18}F-labeled PSMA tracers, such as high edge-contrast, resolution, and signal-to-noise ratio (23).

Here, we present the first clinical study with ^{18}F-JK-PSMA-7 across 10 + 75 patients. As a first step, we showed that distribution patterns of ^{18}F-JK-PSMA-7 and ^{68}Ga-PSMA-11 are highly concordant in patients consecutively examined with the 2 tracers. Interestingly, ^{18}F-JK-PSMA-7 increased the detection rate for suspected lesions in small anatomic structures, such as iliac and retroperitoneal lymph nodes. These lesions might have remained masked by the limited resolution of the ^{68}Ga-emitting tracers, but the detection of such lesions with ^{18}F-JK-PSMA-7 had a substantial impact on subsequent therapy in some of these patients. This finding corroborates our earlier observations on ^{18}F-DCFPyL (7,18). In contrast to our previous studies, however, we were able to observe this improved sensitivity pattern of ^{18}F-JK-PSMA-7 although the acquisition protocol for ^{68}Ga-PSMA-11 had been amended by a second PET scan 3 h after injection for patients

TABLE 1

Patient Characteristics and Localization of Pathologic PSMA Uptake Detected by ^{68}Ga-PSMA-11 PET/CT and ^{18}F-JK-PSMA-7 PET/CT in Initial Cohort of 10 Patients (Patients 1–5)

Patient no.	Age (y)	PSA (ng/mL)	Indication	Gleason score	Dose	PSMA+ Local	PSMA+ Nodal	PSMA+ Distant	Therapeutic consequence	Verification
1	76	1.48*	Taking bicalutamide; intensification of ADT?	4 + 4					Salvage-RT; bicalutamide as before without GnRH analog	PSA decrease to 0.23 ng/mL; M osseous confirmed by previous PET/CT
^{68}Ga-PSMA					160	1	0	0		
^{18}F-JK-PSMA					363	1	0	1		
2	67	0.7	BCR after prostatectomy	4 + 3					RT of upper left iliac LN	PSA decrease to 0.5 ng/mL 4 mo after RT without ADT; after 10 mo PSA 0.6 ng/mL
^{68}Ga-PSMA					172	0	1 left iliac	0		
^{18}F-JK-PSMA					355	0	2 left iliac	0		
3	66	1.03	BCR after prostatectomy and radiotherapy	3 + 4					Wait and see; ^{68}Ga PSMA PET/CT interpreted as unspecific; no indication for LAD or RT	PSA 1.06 ng/mL after 6 mo
^{68}Ga-PSMA					168	0	1 retroperitoneal†	0		
^{18}F-JK-PSMA					347	0	0	0		
4	74	1.1	BCR after prostatectomy	3 + 4					LAD; after progression (PSA, PET/CT) RT of LN area	LN not confirmed by histology (0/4); PSA increase to 2.6 ng/mL after 8 mo; progression proven by external ^{68}Ga-PSMA-11 PET/CT (2 PSMA-positive LN left iliac)
^{68}Ga-PSMA					134	0	0	0		
^{18}F-JK-PSMA					350	0	1 left iliac	0		
5	63	4.7	BCR after prostatectomy	4 + 3					Salvage RT of prostate field	PSA decrease to 0.57 ng/mL
^{68}Ga-PSMA					157	1	0	0		
^{18}F-JK-PSMA					329	1	0	0		

*With ADT.

†Not confirmed by follow-up care.

RT = radiotherapy; GnRH = gonadotropin releasing hormone; M = metastasis; LN = lymph node; LAD = lymphadenectomy; n.a. = not available.

Patient 6 did not receive ^{68}Ga-PSMA-11 PET/CT and was not included in our direct comparison.

TABLE 2
Patient Characteristics and Localization of Pathologic PSMA Uptake Detected by ^{68}Ga-PSMA-11 PET/CT and ^{18}F-JK-PSMA-7 PET/CT in Initial Cohort of 10 Patients (Patients 7–11)

Patient no.	Age (y)	PSA (ng/mL)	Indication	Gleason score	Dose	PSMA+ Local	PSMA+ Nodal	PSMA+ Distant	Therapeutic consequence	Verification
7	52	14.9	BCR after prostatectomy and radiotherapy	3 + 3					^{68}Ga-PSMA PET/CT interpreted as unspecific; no indication for RT of mediastinum	PSMA-negative osteosclerotic bone metastases, detected 9 mo later by ^{68}Ga-PSMA PET/CT
^{68}Ga-PSMA					152	0	2 mediastinal*	0		
^{18}F-JK-PSMA					370	0	0	0		
8	73	0.8	BCR after prostatectomy	4 + 3					Further PSA increase to 1.13 ng/mL; then, RT of retroperitoneal LN area	PSA decrease to 0.42 ng/mL 4 mo after RT without ADT; ^{18}F-PSMA PET/CT (346 MBq) follow-up confirmed at least 2 retroperitoneal PSMA-positive LNs
^{68}Ga-PSMA					129	0	1 retroperitoneal	0		
^{18}F-JK-PSMA					371	0	3 retroperitoneal	0		
9	74	1.017	BCR after prostatectomy	3 + 4					Without any therapy PSA 0.7 ng/mL after 6 mo and 1.2 ng/mL after 8 mo	n.a.
^{68}Ga-PSMA					153	0	0	0		
^{18}F-JK-PSMA					379	0	0	0		
10	59	0.51	BCR after prostatectomy	4 + 3					RT of prostate fossa with regard to R1 and negative PSMA PET scans	PSA decrease to 0.4 ng/mL after 8 mo without ADT
^{68}Ga-PSMA					110	0	0	0		
^{18}F-JK-PSMA					345	0	0	0		
11	69	0.46	BCR after prostatectomy	4 + 3					RT of prostate fossa (standard field)	
^{68}Ga-PSMA					76	1	0	0		
^{18}F-JK-PSMA					370	1	0	0		

*Not confirmed by follow-up care.

RT = radiotherapy; LN = lymph node; n.a. = not available.

Patient 6 did not receive ^{68}Ga-PSMA-11 PET/CT and was not included in our direct comparison.

TABLE 3
Results of ^{18}F-JK-PSMA-7 PET/CT in 75 Patients with BCR, Specified by Initial Therapy and PSA Level

Indication for ^{18}F-JK-PSMA-7 PET/CT	PSMA-negative	PSMA-positive	T+	N+	M+	T+N+	T+M+	N+M+	T+N+M+
BCR or PSA increase after PE ± RT (all)	9	40	10	19	4	1	4	2	
PSA < 0.2 µg/L	1	1		1 (oligo 1)					
BCR, PSA 0.2–0.49 µg/L	4	5	2	3 (oligo 1)					
BCR, PSA 0.5–1.99 µg/L	2	14	2	7 (oligo 6)	3	1	1		
BCR, PSA ≥ 2.0 µg/L	2	20	6	8 (oligo 2)	1		3	2	
BCR or PSA increase after RT (all)	7	19	8	3	3	2	1	1	1
ΔPSA < 2.0 µg/L	6	3	1	1 (oligo 1)	1				
BCR, ΔPSA ≥ 2.0 µg/L	1	16	7	2	2	2 (oligo 1)	1	1	1

T+ = PSMA-positive tissue within prostate fossa; N+ = PSMA-positive lymph node; M+ = PSMA-positive lesion in bone, lung or liver; PE = prostatectomy; RT = radiotherapy; oligo = oligometastasized (here: ≤3 PSMA-positive lymph nodes).

BCR was defined by PSA level of ≥0.2 µg/L after prostatectomy or by increase in PSA level of ≥2.0 µg/L above nadir after radiotherapy. Some patients were sent for ^{18}F-JK-PSMA-7 PET/CT before this criterion was fulfilled and were separately reported.

with PSA levels below 2.0 µg/L (25–28). This finding suggests that the ability of ^{18}F-PSMA–specific ligands to visualize small anatomic structures reflects an intrinsic quality of the ^{18}F label and does not result from differences in image acquisition protocols. It remains an intrinsic advantage of the ^{18}F-labeled PSMA ligands that batches with high ^{18}F activity were produced and that, on each application, the ^{18}F activity injected was higher than the corresponding amount of ^{68}Ga activity.

As a second step, we measured and compared the detection rate of ^{18}F-JK-PSMA-7 in 75 patients with BCR and confirmed that its sensitivity and metastatic pattern also depended largely on the PSA level and type of previous therapy (surgery vs. radiotherapy). The PSA-stratified detection rates that we found for ^{18}F-JK-PSMA-7 in this study were highly concordant with results reported for ^{68}Ga-PSMA-11 by independent institutes with high expertise in this field (4). These observations suggest that the potential sensitivity of the new ^{18}F-JK-PSMA-7 tracer is at least not inferior to previous PSMA tracers. Further, when combining the detection rate of ^{18}F-JK-PSMA-7 across all BCR patients and excluding the patient subgroup with a PSA increase below the Phoenix criterion, we obtained a pooled localization rate of 84.8% (56/66 patients). At the same institute and with the same PET scanner, but in another cohort with the same patient characteristics, we had observed a pooled localization rate of 79.1% (102/129 patients) for ^{68}Ga-PSMA-11 and 74.2% (46/62 patients) for ^{18}F-DCFPyL 2 y ago (18). Indeed, as shown by Mannweiler et al. in immunohistochemical analyses (35), lack of PSMA expression intrinsically limits the sensitivity of PSMA tracers to about 84%, so that ^{18}F-JK-PSMA-7 exploits the full sensitivity potential of PSMA tracers.

Dosimetric data on ^{18}F-JK-PSMA-7 were based on animal studies (23) and then on a cohort of 10 patients (29). ^{18}F-JK-PSMA-7 showed fast excretion via the blood and the kidneys in humans, similar to that seen with ^{18}F-DCFPyL. The blood protein binding of ^{18}F-JK-PSMA-7 was significantly lower than that of ^{18}F-PSMA-1007 and ^{68}Ga-PSMA-11 in animal studies (23). The PSMA-positive metastases in patients showed an increase in SUV$_{max}$ and SUV$_{peak}$ up to 3 h after the injection of ^{18}F-JK-PSMA-7 (29).

Our head-to-head comparison between ^{68}Ga-PSMA-11 and ^{18}F-JK-PSMA-7 had some limitations. It was not designed as a prospective trial. The ^{18}F-JK-PSMA-7 PET scans were clinically indicated by an equivocal or negative interpretation of the first PET scan with ^{68}Ga-PSMA-11 or by an oligometastatic status before radiotherapy. It might be possible that the diagnostic accuracy of ^{68}Ga-PSMA-11 PET/CT was underestimated in the initial cohort of 10 patients. Our working group did not set out to conduct the first-in-humans observational study based on animal studies (23) with testing of ^{18}F-JK-PSMA-7 on healthy volunteers. It is a general advantage of all ^{18}F-labeled PSMA ligands that the injected activities are usually higher than the injected activities of the ^{68}Ga-labeled PSMA ligands. In our pilot study, we injected an activity of approximately 2 MBq of ^{68}Ga-PSMA-11 per kilogram of body weight, which complies with the recommended range for ^{68}Ga-PSMA (1.8–2.2 MBq/kg) in the international guidelines (36), but higher activities of ^{68}Ga-PSMA-11 will have a positive impact on lesion detectability (37).

CONCLUSION

We have shown that ^{18}F-JK-PSMA-7 is safe and that its sensitivity in prostate cancer patients is not inferior to that of ^{68}Ga-PSMA-11. Further, in parallel with previous studies with ^{18}F-DCFPyL, we observed even improved sensitivity for ^{18}F-JK-PSMA-7, a modified version of ^{18}F-DCFPyL, compared with ^{68}Ga-PSMA-11 in a few selected patients with PSMA-positive lesions in small lymph nodes. Additionally, the simplicity, high radiochemical yield, and robustness of ^{18}F-JK-PSMA-7 production propose use of this PSMA-specific agent for routine clinical diagnostics.

DISCLOSURE

KEY POINTS

QUESTIONS: Is ^{18}F-JK-PSMA-7, a modified version of ^{18}F-DCFPyL, helpful for PET/CT imaging of patients with prostate cancer?

PERTINENT FINDINGS: ^{18}F-JK-PSMA-7 was directly compared with ^{68}Ga-PSMA-11 PET/CT in a pilot study including 10 patients, and additional suspected PSMA-positive lesions were identified in 4 patients. During the first year of application, ^{18}F-JK-PSMA-7 PET/CT detected at least 1 PSMA-positive lesion in 84.8% of the patients with BCR.

IMPLICATIONS FOR PATIENT CARE: We observed an improved detection rate for ^{18}F-JK-PSMA-7 compared with ^{68}Ga-PSMA-11 in a few selected patients with PSMA-positive lesions in small lymph nodes.

REFERENCES

1. Artibani W, Porcaro AB, De Marco V, Cerruto MA, Siracusano S. Management of biochemical recurrence after primary curative treatment for prostate cancer: a review. *Urol Int.* 2018;100:251–262.

2. Han S, Woo S, Kim YJ, Suh CH. Impact of ^{68}Ga-PSMA PET on the management of patients with prostate cancer: a systematic review and meta-analysis. *Eur Urol.* 2018;74:179–190.

3. Afshar-Oromieh A, Avtzi E, Giesel FL, et al. The diagnostic value of PET/CT imaging with the ^{68}Ga-labelled PSMA ligand HBED-CC in the diagnosis of recurrent prostate cancer. *Eur J Nucl Med Mol Imaging.* 2015;42:197–209.

4. Eiber M, Maurer T, Souvatzoglou M, et al. Evaluation of hybrid ^{68}Ga-PSMA ligand PET/CT in 248 patients with biochemical recurrence after radical prostatectomy. *J Nucl Med.* 2015;56:668–674.

5. Bluemel C, Krebs M, Polat B, et al. ^{68}Ga-PSMA-PET/CT in patients with biochemical prostate cancer recurrence and negative ^{18}F-choline-PET/CT. *Clin Nucl Med.* 2016;41:515–521.

6. Szabo Z, Mena E, Rowe SP, et al. Initial evaluation of [^{18}F]DCFPyL for prostate-specific membrane antigen (PSMA)-targeted PET imaging of prostate cancer. *Mol Imaging Biol.* 2015;17:565–574.

7. Dietlein M, Kobe C, Kuhnert G, et al. Comparison of [^{18}F]DCFPyL and [^{68}Ga]Ga-PSMA-HBED-CC for PSMA-PET imaging in patients with relapsed prostate cancer. *Mol Imaging Biol.* 2015;17:575–584.

8. Giesel FL, Hadaschik B, Cardinale J, et al. F-19 labelled PSMA-1007: biodistribution, radiation dosimetry and histopathological validation of tumor lesions in prostate cancer patients. *Eur J Nucl Med Mol Imaging.* 2017;44:678–688.

9. Rahbar K, Afshar-Oromieh A, Seifert R, et al. Diagnostic performance of ^{18}F-PSMA-1007 PET/CT in patients with biochemical recurrent prostate cancer. *Eur J Nucl Med Mol Imaging.* 2018;45:2055–2061.

10. O'Keefe DS, Su SL, Bacich DJ, et al. Mapping, genomic organization and promoter analysis of the human prostate-specific membrane antigen gene. *Biochim Biophys Acta.* 1998;1443:113–127.

11. O'Keefe DS, Bacich DJ, Heston WD. Comparative analysis of prostate-specific membrane antigen (PSMA) versus a prostate-specific membrane antigen-like gene. *Prostate.* 2004;58:200–210.

12. Afshar-Oromieh A, Debus N, Uhrig M, et al. Impact of long-term androgen deprivation therapy on PSMA ligand PET/CT in patients with castration-sensitive prostate cancer. *Eur J Nucl Med Mol Imaging.* 2018;45:2045–2054.

13. Armstrong IS, Kelly MD, Williams HA, Matthews JC. Impact of point spread function modelling and time of flight on FDG uptake measurements in lung lesions using alternative filtering strategies. *EJNMMI Phys.* 2014;1:99.

14. Jacobson O, Kiesewetter DO, Chen X. Fluorine-18 radiochemistry, labeling strategies and synthetic routes. *Bioconjug Chem.* 2015;26:1–18.

15. Banerjee SR, Pullambhatla M, Byun Y, et al. ^{68}Ga-labeled inhibitors of prostate-specific membrane antigen (PSMA) for imaging prostate cancer. *J Med Chem.* 2010;53:5333–5341.

16. Berry DJ, Ma Y, Ballinger JR, et al. Efficient bifunctional gallium-68 chelators for positron emission tomography: tris(hydroxypyridinone) ligands. *Chem Commun (Camb).* 2011;47:7068–7070.

17. Chen Y, Pullambhatla M, Foss CA, et al. 2-(3-{1-carboxy-5-[(6-[^{18}F]fluoro-pyridine-3-carbonyl)-amino]-pentyl}-ureido)-pentanedioic acid, [^{18}F]DCFPyL, a PSMA-based PET imaging agent for prostate cancer. *Clin Cancer Res.* 2011;17:7645–7653.

18. Dietlein F, Kobe C, Neubauer S, et al. PSA-stratified performance of [18]F- and ^{68}Ga-PSMA PET in patients with biochemical recurrence of prostate cancer. *J Nucl Med.* 2017;58:947–952.

19. Gorin MA, Rowe SP, Patel HD, et al. Prostate specific membrane antigen targeted ^{18}F-DCFPyL positron emission tomography/computerized tomography for the preoperative staging of high risk prostate cancer: results of a prospective, phase II, single center study. *J Urol.* 2018;199:126–132.

20. Bouvet V, Wuest M, Jans HS, et al. Automated synthesis of [^{18}F]DCFPyL via direct radiofluorination and validation in preclinical prostate cancer models. *EJNMMI Res.* 2016;6:40.

21. Ravert HT, Holt DP, Chen Y, et al. An improved synthesis of the radiolabeled prostate-specific membrane antigen inhibitor, [^{18}F]DCFPyL. *J Labelled Comp Radiopharm.* 2016;59:439–450.

22. Robu S, Schmidt A, Eiber M, et al. Synthesis and preclinical evaluation of novel ^{18}F-labeled Glu-urea-Glu-based PSMA inhibitors for prostate cancer imaging: a comparison with ^{18}F-DCFPyl and ^{18}F-PSMA-1007. *EJNMMI Res.* 2018;8:30.

23. Zlatopolskiy BD, Endepols H, Krapf P, et al. Discovery of ^{18}F-JK-PSMA-7, a novel PET-probe for the detection of small PSMA positive lesions. *J Nucl Med.* 2019;60:817–823.

24. Wondergem M, van der Zant FM, Vlottes PW, Knol RJJ. Effects of fasting on ^{18}F-DCFPyL uptake in protate cancer lesions and tissues with known high physiologic uptake. *J Nucl Med.* 2018;59:1081–1084.

25. Schmuck S, Nordlohne S, von Klot CA, et al. Comparison of standard and delayed imaging to improve the detection rate of [^{68}Ga]PSMA I&T PET/CT in patients with biochemical recurrence or prostate-specific antigen persistence after primary therapy for prostate cancer. *Eur J Nucl Med Mol Imaging.* 2017;44:960–968.

26. Afshar-Oromieh A, Sattler LP, Mier W, et al. The clinical impact of additional late PET/CT imaging with ^{68}Ga-PSMA-11 (HBED-CC) in the diagnosis of prostate cancer. *J Nucl Med.* 2017;58:750–755.

27. Derlin T, Weiberg D, von Klot C, et al. ^{68}Ga-PSMA I&T PET/CT for assessment of prostate cancer: evaluation of image quality after forced diuresis and delayed imaging. *Eur Radiol.* 2016;26:4345–4353.

28. Hohberg M, Kobe C, Täger P, et al. Combined early and late [^{68}Ga]Ga-PSMA-HBED-CC PET scans improve lesion detectability in biochemical recurrence of prostate cancer with low PSA levels. *Mol Imaging Biol.* 2019;21:558–566.

29. Hohberg M, Dietlein M, Kobe C, et al. Biodistribution and radiation dosimetry of the novel ^{18}F-labeled prostate-specific membrane antigen-ligand PSMA-7 for PET/CT in prostate cancer patients [abstract]. *J Nucl Med.* 2018;59(suppl 1):88.

30. Eiber M, Herrmann K, Calais J, et al. Prostate cancer molecular imaging standardized evaluation (PROMISE): proposed miTNM classification for the interpretation of PSMA-ligand PET/CT. *J Nucl Med.* 2018;59:469–478.

31. Rowe SP, Pienta KJ, Pomper MG, Gorin MA. Proposal for a structured reporting system for prostate-specific membrane antigen-targeted PET imaging: PSMA-RADS version 1.0. *J Nucl Med.* 2018;59:479–485.

32. Eder M, Schafer M, Bauder-Wust U, et al. ^{68}Ga-complex lipophilicity and the targeting property of a urea-based PSMA inhibitor for PET imaging. *Bioconjug Chem.* 2012;23:688–697.

33. Schäfer M, Bauder-Wust U, Leotta K, et al. A dimerized urea-based inhibitor of the prostate-specific membrane antigen for ^{68}Ga-PET imaging of prostate cancer. *EJNMMI Res.* 2012;2:23.

34. Hammes J, Hohberg M, Täger P, et al. Uptake in non-affected bone tissue does not differ between [^{18}F]-DCFPyL and [^{68}Ga]-HBED-CC PSMA PET/CT. *PLoS One.* 2018;13:e0209613.

35. Mannweiler S, Amersdorfer P, Trajanoski S, Terrett JA, King D, Mehes G. Heterogeneity of prostate-specific membrane antigen (PSMA) expression in prostate carcinoma with distant metastasis. *Pathol Oncol Res.* 2009;15:167–172.

36. Fendler WP, Eiber M, Beheshti M, et al. ^{68}Ga-PSMA PET/CT: joint EANM and SNMMI procedure guideline for prostate cancer imaging: version 1.0. *Eur J Nucl Med Mol Imaging.* 2017;44:1014–1024.

37. Rauscher I, Fendler WP, Hope T, et al. Image quality and lesion detectability using different simulated activities of ^{68}Ga-PSMA.11 [abstract]. *Nucl Med (Stuttg).* 2019;58(suppl):150–151.